Systems pharmacology and blood-brain barrier functionality in Parkinson's disease

Ravenstijn, P.G.M.

Chapter 5

The Intracerebral Rotenone Model of Parkinson's Disease in Rats:

Altered Conversion of L-DOPA into DOPAC and HVA without Changes in BBB Transport

PGM Ravenstijn[1], H Drenth[2], MS Baatje[1], MJ O'Neill[3], M Danhof[1] and ECM de Lange[1]

[1] LACDR, Division of Pharmacology, Leiden University, Leiden, The Netherlands

[2] LAP&P Consultants BV, Leiden, The Netherlands

[3] Eli Lilly & Co Ltd, Neurodegeneration Drug Hunting Team, Windlesham, UK

Abstract

The aim was to study the pharmacokinetics (PK) and blood-brain barrier (BBB) transport in conjunction with the conversion of L-DOPA into DOPAC and HVA in the rat rotenone model of Parkinson's disease.

Male Lewis rats were unilaterally infused with rotenone in the medial forebrain bundle (MFB). The contralateral side served as a control. After 14 days, L-DOPA (10, 25 or 50 mg/kg) was intravenously infused. Blood samples and brain striatal microdialysates were collected and analysed. Brains were histologically evaluated on tyrosine hydroxylase staining to identify responders and non-responders. Population PK analysis was performed by NONMEM to determine the influence of the Parkinson's disease state on plasma PK, BBB transport of L-DOPA and DOPAC and HVA levels in the brain.

Rotenone infusion resulted in 71% of the rats developing neurostriatal degeneration. The plasma PK of L-DOPA could be adequately described by a 3-compartmental model. No difference was observed between BBB transport of L-DOPA in lesioned and untreated brain side. DOPAC and HVA basal microdialysate levels were substantially lower in the lesioned striatum, while also, following L-DOPA administration, their elimination rates were higher in lesioned striatum.

Our study demonstrates that Parkinson's disease-like pathology induced by rotenone does not result in changes in the kinetics and BBB transport of L-DOPA. Merely, a clear effect of disease on the levels and elimination rates of DOPAC and HVA in brain were found, providing information on decreased dopamine concentrations at the lesioned brain side.

1. Introduction

Parkinson's disease is a progressive neurodegenerative disease in which dopamine-producing cells in the nigrostriatal pathway are affected. The chronic and progressive decrease in dopamine concentration in the striatum leads to the development of the classic symptoms of Parkinson's disease, such as tremor, rigidity and bradykinesia (Dauer and Przedborski, 2003). The current therapies of Parkinson's disease are mainly focussed on symptomatic treatment by replacing the striatal dopamine (Factor, 2008; Nyholm, 2006; Savitt *at al.*, 2006; Schapira, 2008). Among the antiparkinson drugs available, L-3,4-dihydroxyphenylalanine (L-DOPA) is still considered the most efficacious treatment of Parkinson's symptoms (Deleu *at al.*, 2002; Factor, 2008; Nyholm, 2006; Schapira, 2008).

To investigate the mechanisms of action of antiparkinsonian drugs, one would like to use a preclinical Parkinson's disease model that allows for investigation at different stages of the disease. In **chapter 4**, we have explored the intracerebral rotenone rat model for Parkinson's disease, which showed to be capable of producing a relatively slow progressive degeneration of the nigrostriatal system and was associated with the formation of inclusion bodies similar to that observed in Parkinson's disease (Ravenstijn *at al.*, 2008).

The goal of this study was to determine the PK in plasma, BBB transport, and within-brain conversion of L-DOPA into dopamine and its major metabolites DOPAC and HVA in this rat model for Parkinson's disease. The microdialysis technique (de Lange *at al.*, 1999; Hammarlund-Udenaes, 2000) was used to measure free L-DOPA, dopamine, DOPAC and HVA concentrations. To examine the influence of Parkinson's disease, two microdialysis probes were inserted in the lesioned side and in the contralateral healthy side of the brain respectively. Microdialysates were collected in parallel with serial blood samples. Concentrations of the compounds were determined under basal conditions and following *i.v.* administration of 10, 25 and 50 mg/kg of L-DOPA. At the end of the experiment brains were removed for immunostaining on tyrosine hydroxylase (TH) to determine responders and non-responders on the basis of the percentage loss of dopaminergic terminals in the striatum in control and rotenone-infused rats. A compartmental, population-based analysis was performed to determine the influence of the Parkinson's disease state on plasma PK, BBB transport of L-DOPA and DOPAC and HVA levels in the brain.

2. Materials and Methods

All animal procedures described in this paper were approved by the Ethical Committee on Animal Experimentation of the University of Leiden (DEC numbers 118 and 5069).

Animals and surgical procedures

Experiments were performed on male Lewis rats (Charles River BV, Maastricht, The Netherlands) weighing 311 ± 17g (mean ± s.d., n=18) and 288 ± 13g (mean ± s.d., n=17) before surgery and before start of the experiment, respectively. The rats were housed in standard plastic cages (six per cage before surgery and individually after surgery) with a 12-hour day/night schedule (lights on 7:30 AM) and at a temperature of 21°C.

The animals had access to standard laboratory chow (RMH-TM; Hope Farms, Woerden, The Netherlands) and acidified water *ad libitum*.
The surgery was performed under anesthesia with an intramuscular injection of 0.1 mg/kg medetomidine hydrochloride (Domitor 1 mg/ml, Pfizer, Capelle a/d IJssel, The Netherlands) and 1 mg/kg ketamine base (Ketalar 50 mg/ml, Parke-Davis, Hoofddorp, The Netherlands). Three indwelling cannulas (pyrogen-free, nonsterile polyethylene tubing, Portex Limited) were implanted, one in the left femoral artery (for blood sampling) and two in the left femoral vein (for drug administration). The cannulas were tunnelled subcutaneously and fixed at the back of the neck with a rubber ring. The skin in the neck was stitched with normal sutures. The skin in the groin was closed with wound clips. To prevent clotting and cannula obstruction, the cannulas were filled with a 25% (w/v) polyvinylpyrrolidone solution (PVP; Brocacef, Maarssen, The Netherlands) in pyrogen-free physiological saline (B. Braun Melsungen AG, Melsungen, Germany) containing 20 IU/ml heparin (Hospital Pharmacy, Leiden University Medical Center, Leiden, The Netherlands).

After the implantation of the blood cannulas, the rats were placed in a stereotaxic frame and the skull was exposed for brain surgery. The skull was cleaned and a hole was burred to allow a needle to be lowered into the right median forebrain bundle (MFB: AP: -2.8; L: +2.0; V: -9.0 relative to bregma (Paxinos *at al.*, 1985)) for unilateral infusion of 5.0 µg of rotenone (Rotenone Pestanal ; Sigma Alldrich BV, Zwijndrecht, the Netherlands) at a rate of 0.1 µl/min for 30 minutes. Rotenone was dissolved in a 1:1-mixture of dimethylsulfoxide (DMSO, Sigma Alldrich BV, Zwijndrecht, the Netherlands) with polyethylene glycol (PEG 200, Sigma Alldrich BV, Zwijndrecht, the Netherlands). After the infusion, the needle was kept in place for another 5 minutes to allow diffusion of the fluid without leakage along the track of the needle. Subsequently, two small holes were drilled into the skull to allow implantation of a microdialysis guide cannula (CMA/12, Aurora Borealis Control B.V. Schoonebeek, The Netherlands) in the left and in the right striatum (AP: +0.4; L: +/-3.2; V: -3.5, relative to bregma; (Paxinos *at al.*, 1985)). One support screw was placed as an extra anchor for fixation of the guide, which was glued to the skull with dental acrylic cement (Howmedia simplex rapid + methylacrylate, Drijfhout, Amsterdam, The Netherlands). After surgery, the rats were assigned to one of three dosing groups (n=6 per group). The microdialysis experiment was carried out 14 days after surgery. The details of the intracerebral rotenone model have been described in **Chapter 4**.

Microdialysis

At 13 days after the unilateral infusion of rotenone into the right MFB, and 18-24 hours prior to the experiment, the microdialysis probes (CMA12, membrane length of 4.0 mm; Aurora Borealis Control B.V. Schoonebeek, the Netherlands) were inserted into the guide cannulas. All animals were fasted overnight prior to the experiment in order to rule out any competition in BBB transport of L-DOPA with food-related amino acids (Nutt *at al.*, 1984).

The microdialysis experiment, 14 days post rotenone treatment, was started between 7:00 and 8:00 a.m. The inlets of the microdialysis probes were connected by FEP tubing (fluorinated ethylene propylene tubing; Aurora Borealis Control B.V. Schoonebeek, the Netherlands) to syringe pumps (Beehive, Bas Technicol, Congleton, United Kingdom). The probes were perfused with artificial ECF (composition in mM: NaCl 145; KCl 2.7; CaCl2 1.2; MgCl2 1.0; ascorbic acid 0.2 in a 2 mM phosphate buffer pH 7.4; (Moghaddam and Bunney, 1989)) at a flow rate of 2 µl/min. The outlets also consisted of FEP tubing and were connected to a microsample collector (Univentor 820; Antec, Leiden, The Netherlands), in which the samples were collected at 4ºC. The vials contained an antioxidant fluid (0.1 M acetic acid, 3.3 mM L-cysteine, 0.27 M EDTA, 0.0125 mM ascorbic acid dissolved in millipore water) in a ratio of 1:4 with the expected volume of the microdialysate to prevent the breakdown of the catecholamines. After a stabilisation period of 60 minutes, the *in vivo* recovery of L-DOPA was determined by the retrodialysis method. For this purpose, the probes were perfused with a L-DOPA solution (10, 100 or 200 ng/ml for the 10, 25 and 50 mg/kg dose group, respectively) for 60 minutes to collect 6 fractions. The relative loss of L-DOPA was used for estimating $brain_{ECF}$ concentrations. After the retrodialysis, the syringes were switched to blank perfusion fluid for a washout phase of 90 minutes. After the washout period, the intravenous administration of L-DOPA was started. One venous cannula was connected to a syringe containing L-DOPA (Sigma Alldrich BV, Zwijndrecht, the Netherlands) in 0.2 M HCl in saline (0.9% NaCl) and ascorbic acid (5% of the L-DOPA amount) and the second venous cannula was connected to a syringe containing 7% $NaHCO_3$ (to neutralise the acidic L-DOPA solution). Both infusions were started at the same time for 20 minutes at a rate of 20 µl/min. In the first 120 minutes of the experiment, microdialysis fractions were collected at 10-minute intervals. From 120-180 minutes, microdialysis fractions were collected at 20-minute intervals. From 180 minutes until the end of the experiment (360 minutes), microdialysis fractions were collected at 30-minute intervals. Blood samples (50 µl in heparinised Eppendorf vials) were taken predose and at 5, 10,

15, 20, 22, 24, 26, 28, 30, 45, 50, 60, 75, 90, 120, 180, 240, 360 minutes after start of the L-DOPA infusion. The blood samples were centrifuged for 10 minutes at 5000 rpm and the plasma was pipetted into Eppendorf vials. All samples were stored at -80 C before analysis. After the experiment, the animals were given an overdose of sodium pentobarbital (Nembutal, Ceva Santa Animale, Maassluis, The Netherlands) and the thorax was opened and the vascular bed was perfused via the left ventricle of the heart with 30 ml of saline followed by 30 ml of 10% phosphate buffered formalin (pH 7.0). Brains were removed for histopathology.

Immunohistopathology

TH immunohistochemistry was performed to quantify the degree of dopaminergic depletion as described previously in **Chapter 4**. The percentage of intact TH staining in the rotenone-treated hemisphere was calculated as the percentage of striatal MGV compared to the striatal MGV of the untreated hemisphere. In the clinical setting, symptoms of Parkinson's disease arise when about 80% of striatal dopamine and about 60% of dopamine neurons are lost (Dauer and Przedborski, 2003). Therefore, the rats which failed to show significant loss in TH staining were considered as 'non-responders' to the rotenone treatment.

Bioanalysis of L-DOPA, DOPAC and HVA

All plasma samples were analysed for L-DOPA and all microdialysate samples were analysed for L-DOPA, dopamine, DOPAC and HVA using a high performance liquid chromatography (HPLC) system with electrochemical detection (ECD).

HPLC and ECD system

The HPLC system consisted of a LC-10AD HPLC pump (Shimadzu, 's Hertogenbosch, The Netherlands), a Waters 717 Plus autosampler (Waters, Etten-Leur, The Netherlands), a pulse damper (Antec Leyden, Zoeterwoude, The Netherlands) and a digital electrochemical amperometric detector (DECADE, software version 3.02, Antec Leyden, Zoeterwoude, The Netherlands). The electrochemical detector consisted of a VT-03 electrochemical flow cell combined with a 25 µm spacer and an *in situ* Ag/AgCl (ISAAC) reference electrode operating in the DC mode. For the analysis, a standard Ag/AgCl reference electrode, filled with a saturated KCl solution was used. Data acquisition and processing was performed using the Empower® data-acquisition software (Waters, Etten-Leur, The Netherlands).

Bioanalysis in plasma

Chromatography of plasma samples of L-DOPA was performed on a Beckman Coulter™ Ultrasphere® 5 µm C-18 column (4.6 mm I.D. x 150 mm, Alltech, Breda, The Netherlands) equipped with a refill guard column (2 mm I.D. x 20 mm, Upchurch Scientific, Oak Harbor, WA, USA) packed with pellicular C18 material (particle size 20-40 µm, Alltech, Breda, The Netherlands) at a constant temperature of 30°C. The mobile phase was a mixture of 0.05 M sodium phosphate buffer (pH 2.8) and methanol (90:10, v/v), supplemented with 0.3 mM EDTA (sodium salt) and 10 mM octane-sulfonic acid. Before the addition of methanol, the mobile phase was filtered through a 0.2 µm nylon filter (Alltech, Breda, The Netherlands), then the methanol was added and it was mixed and degassed with helium. The flow rate was set at 1 mL/min. The optimal working potential for L-DOPA was +0.75 V, as determined by a voltammogram and sensitivity plot. Concentrations were measured at a sensitivity range of 5 nA for L-DOPA and 20 nA for 3,4-dihydroxybenzylamine hydrobromide (DHBA; internal standard). Stock solutions of L-DOPA were prepared at a concentration of 1 mg/mL in Millipore water. The stock solutions were diluted with Millipore water to obtain calibration solutions in the range of 2 to100 ng/mL. The internal standard (DHBA) solution was prepared by dilution of the stock solution to a final concentration of 500 ng/mL. The stock solutions were stored at -80 °C up to one month. The assay solutions were prepared freshly before each analysis. For determination of the L-DOPA in plasma, 25 µL of internal standard solution (DHBA 500 ng/mL) was added to 45 µL plasma samples and 50 µL of Millipore water in glass centrifuge tubes. Next, 25 µL of 20% TCA was added and the mixture was vortexed for 5 min. After centrifugation for 10 min at 4000 rpm (2000g), 100 µL of the supernatant was added to 50 µL of phosphoric buffer (1M, pH 5.5) of which 25 µL was injected into the HPLC system.

Bioanalysis in microdialysate

For analysis of L-DOPA, dopamine, DOPAC and HVA brain microdialysate concentrations, 5 µL of internal standard (isoproterenol; 100 ng/mL) solution was added per 10 µL of microdialysis sample or calibration curve sample. The samples were then injected (20 µL) into the HPLC system without further sample pre-treatment. Chromatography of brain microdialysate samples was performed on a Beckman Coulter™ Ultrasphere® 5 µm C-18 column (2 mm I.D. x 250 mm, Alltech, Breda, The Netherlands) at a constant temperature of 30 °C. The mobile

phase was a mixture of 0.05 M sodium phosphate buffer (pH 2.8) and methanol (88:12, v/v), supplemented with 0.3 mM EDTA (sodium salt) and 1.5 mM octane-sulfonic acid. Mobile phase solvents were filtered through a 0.2 µm nylon filter. Then, the methanol was added and the mobile phase was mixed and degassed with helium. The flow rate was set at 0.2 mL/min. The optimal working potential for a mixture of L-DOPA, dopamine, DOPAC and HVA was +0.66 V, as determined by a voltammogram and sensitivity plot. Concentrations were measured at a sensitivity range of 0.1 nA for dopamine, 0.5 nA for L-DOPA, HVA and isoproterenol; and 10 nA for DOPAC. For analysis of brain microdialysate samples, stock solutions of L-DOPA, DOPAC and HVA were prepared at a concentration of 0.5 µg/mL for dopamine, 1 µg/mL for L-DOPA and 5 µg/mL for DOPAC and HVA in microdialysis perfusion fluid with aqueous antioxidant solution consisting of 0.1 M acetic acid, 3.3 mM L-cysteine, 0.27 M EDTA (sodium salt) and 0.0125 mM ascorbic acid (4:1 v/v). Internal standard solution was prepared fresh before each analysis by dilution of a 1 mg/mL isoproterenol stock solution to 100 ng/mL perfusion fluid with antioxidant (4:1 v/v). All the stock solutions were stored at -80 °C up to one month. Before each analysis a first calibration solution containing all compounds was freshly prepared by mixing one volume part of each compounds' stock solution (L-DOPA, dopamine, DOPAC and HVA) and adding 5 volume parts of perfusion fluid with antioxidant (4:1 v/v). This first calibration solution now contained all compounds at a concentration 10 times lower than their stock solution and from this solution the other calibration solutions were prepared.

Population pharmacokinetic analysis

The pharmacokinetics of L-DOPA, DOPAC and HVA were analysed utilizing a population PK modelling approach. Dopamine concentrations were all below the limit of detection. Compartmental modelling was performed using the ADVAN6 subroutine in NONMEM VI release 2 (GloboMax LLC, Hanover, MD, USA). All fitting procedures were performed on an IBM-compatible computer (Pentium IV, 1500 MHz) running under Windows XP with the Compaq Visual Fortran compiler version 6.6.

The inter-individual variability of model parameters was described by an exponential equation, according to:

$$P_{1i} = \theta_1 * exp(\eta_i),$$

where θ_1 is the population (typical) estimate for parameter P_1, P_{1i} is the individual estimate and η_i determines the random deviation of P_{1i} from P_1. The values of η_i are assumed to be randomly, normally distributed with mean zero and variance ω_{11}^2. The residual error in the L-DOPA concentration was described by a proportional error model:

$$C_{obs,ij} = C_{pred,ij} * (1+\varepsilon_{ij}),$$

and the residual error in the DOPAC or HVA concentration was described by an additive error model:

$$C_{obs,ij} = C_{pred,ij} + \varepsilon_{ij}$$

where $C_{obs,ij}$ represents the j^{th} measured L-DOPA, DOPAC or HVA concentration for the i^{th} individual predicted by the model. $C_{pred,ij}$ represents the prediction of concentration and ε_{ij} is the deviation of the model-predicted value from the observed concentration. The values of ε are assumed to be randomly, normally distributed with mean zero and variance σ^2. The first order conditional estimation method with interaction (FOCE interaction) was used in NONMEM to fit the models to the data and to estimate θ's, ω^2's and σ^2's.

Structural model selection for all models was based on the likelihood ratio test, diagnostic plots (observed concentrations vs. individual and population predicted concentrations, conditional weighted residuals vs. time and predicted concentrations), parameter correlations and precision in parameter estimates. Inclusion of one parameter into the model was assumed to be significant if this led to a decrease of 10.8 points or more of the minimum value of the objective function (MVOF) after fitting the model to the data. This corresponds to a theoretical significance level of p=0.001 under the assumption that the difference in MVOF between two nested models is χ^2 distributed.

In total, the L-DOPA plasma profiles of 13 rats (10 mg/kg: n=4; 25 mg/kg: n=4; 50 mg/kg: n=5) and the L-DOPA $brain_{ECF}$ profiles from the untreated brain side of 12 rats (10 mg/kg: n=4; 25 mg/kg: n=3; 50 mg/kg: n=5) and the L-DOPA $brain_{ECF}$ profiles from the lesioned brain side of 7 rats (10 mg/kg: n=1; 25 mg/kg: n=2; 50

mg/kg: n=4) were included in the population PK analysis. On the basis of selection criteria, the plasma and brain$_{ECF}$ L-DOPA data from all individual rats were simultaneously analysed (Figure 1). Individual model parameters (*post hoc* estimates) for each animal from this analysis and typical values from this model (Table 1) were then used as input for the subsequent analysis of DOPAC (Figure 1; compartments 6 and 8) and HVA (Figure 1; compartments 7 and 9). In total, the DOPAC and HVA microdialysate concentrations from the healthy/untreated brain side of 12 rats (10 mg/kg: n=4; 25 mg/kg: n=3; 50 mg/kg: n=5) and the DOPAC and HVA microdialysate concentrations from the lesioned brain side of 8 rats (10 mg/kg: n=2; 25 mg/kg: n=2; 50 mg/kg: n=4) were included in the population PK analysis.

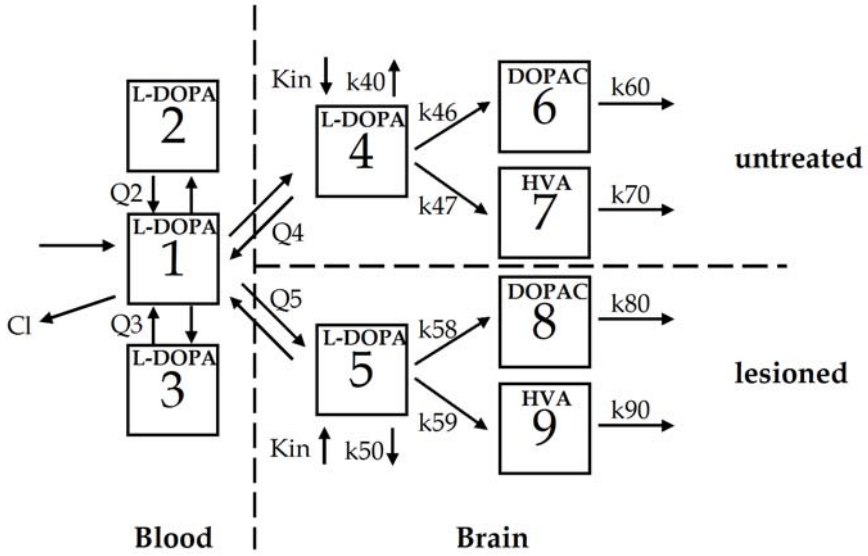

Figure 1: *The population pharmacokinetic model for L-DOPA, DOPAC and HVA comprising of three compartments (1-3) describing the PK of L-DOPA in plasma, two compartments (4 & 5) describing the PK of L-DOPA in brain$_{ECF}$, one for the untreated brain side and one for the lesioned brain side, two compartments (6 & 8) describing the PK of DOPAC in brain$_{ECF}$, one for the untreated brain side and one for the lesioned brain side and two compartments (7 & 9) describing the PK of HVA in brain$_{ECF}$, one for the untreated brain side and one for the lesioned brain side.*

3. Results

General

The percentage of intact TH staining in the rotenone-treated hemisphere compared to the untreated hemisphere was below 40% in 12 out of 17 rats, and higher than 90% in the remaining 5 rats. The rats which exhibited a TH staining level lower than 40% (60-100% of the dopamine terminals were lost) were considered as 'responders' to the rotenone treatment and those brain sides were considered as diseased (lesioned).

No quantifiable concentrations of dopamine could be detected throughout the experiment (LOQ of 0.01 ng/mL in a 20 µl microdialysate sample). As a consequence, dopamine concentrations were not included in the data analysis.

A total of 17 rats (n=6 in the 10- and 25 mg/kg dose group and n=5 in the 50 mg/kg dose group) were used in the microdialysis experiments. All microdialysate concentrations of L-DOPA were corrected for the average *in vivo* recovery as determined during the retrodialysis period (30 ± 6 %) in order to estimate brainECF concentrations. The *in vivo* recovery was equal for the three concentrations of L-DOPA used.

Data analysis

L-DOPA pharmacokinetic modelling

The individual plasma concentration-time profiles following intravenous infusion of L-DOPA are shown in Figure 2. The individual $brain_{ECF}$ concentration-time profiles are shown in Figure 3. The L-DOPA in plasma and in $brain_{ECF}$ (both lesioned and untreated brain sides) were analysed simultaneously. All structural parameters of the population PK model for L-DOPA could be adequately estimated (Table 1). The goodness-of-fit plots for L-DOPA are depicted in Figure 4. No dose-dependency was observed in the plasma PK for L-DOPA.

No significant difference could be detected between the inter-compartmental clearances Q4 and Q5, the volumes of distribution V4 and V5 or the elimination rate constants k40 and k50 when these models were fitted to the L-DOPA brain concentration data. Table 2 shows a summary of the MVOF and parameters estimates after the different assumptions (Q4=Q5, V4=V5, k40=k50 or a combination of any of these assumptions). Also, the separate estimation of endogenous brain production rate of L-DOPA (Kin) for compartment 4 and 5 resulted in similar estimated values (5.8 min^{-1}). Striatal microdialysate baseline L-DOPA levels in the lesioned brain sides were insignificantly lower (P-value=0.07; Welch's t-test) than in the untreated brain side and averaged

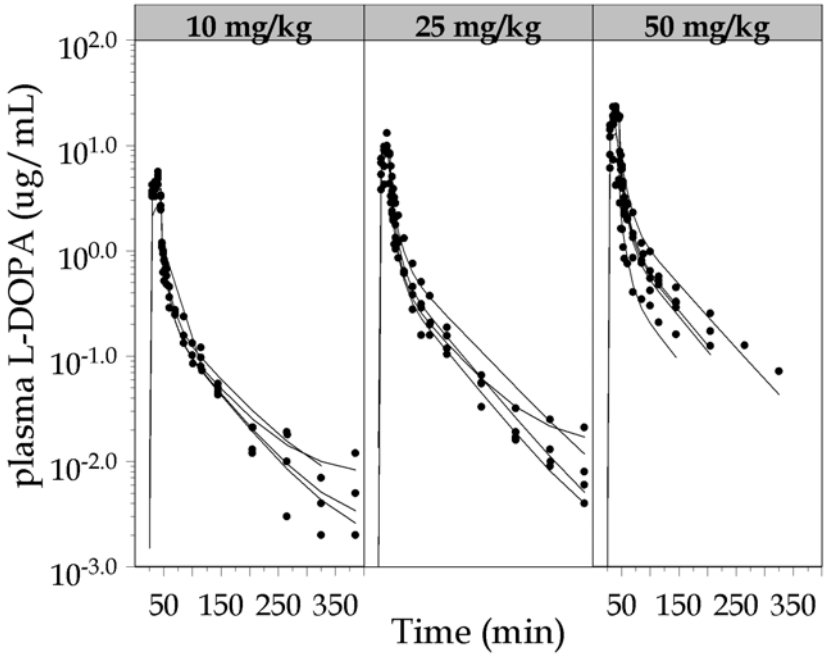

Figure 2: *L-DOPA concentration-time profiles in plasma, obtained after a 20-min i.v. infusion in Lewis rats. Depicted are the observed concentrations (dots), individual predictions (solid lines), separated by L-DOPA dose (in total 13 rats: 10 mg/kg: n=4; 25 mg/kg: n=4; 50 mg/kg: n=5).*

0.010 ± 0.004 pmol/mL and 0.024 ± 0.011 pmol/mL (mean ± SEM), respectively. Therefore, it can be concluded that no significant difference can be identified between the PK of L-DOPA in the untreated brain side *versus* the lesioned brain side.

DOPAC and HVA kinetic modelling

Striatal microdialysate baseline DOPAC levels in the lesioned brain side were about 6 times lower than in the untreated brain side and averaged 0.2 ± 0.19 pmol/mL and 1.3 ± 0.17 pmol/mL (mean ± SEM), respectively (P-value<0.01; Welch's t-test). Also, striatal microdialysate baseline HVA levels in the lesioned brain side were lower (approximately 4 times) than in the healthy brain side and averaged 0.25 ± 0.14 pmol/mL and 0.9 ± 0.08 pmol/mL (mean ± SEM), respectively (P-value=0.02; Welch's t-test). Figure 5 shows the population predicted microdialysate concentrations of DOPAC and HVA versus time for a typical rat per dose group. The goodness-of-fit plots for DOPAC and HVA in microdialysate are depicted in Figure 6. All structural parameters of the

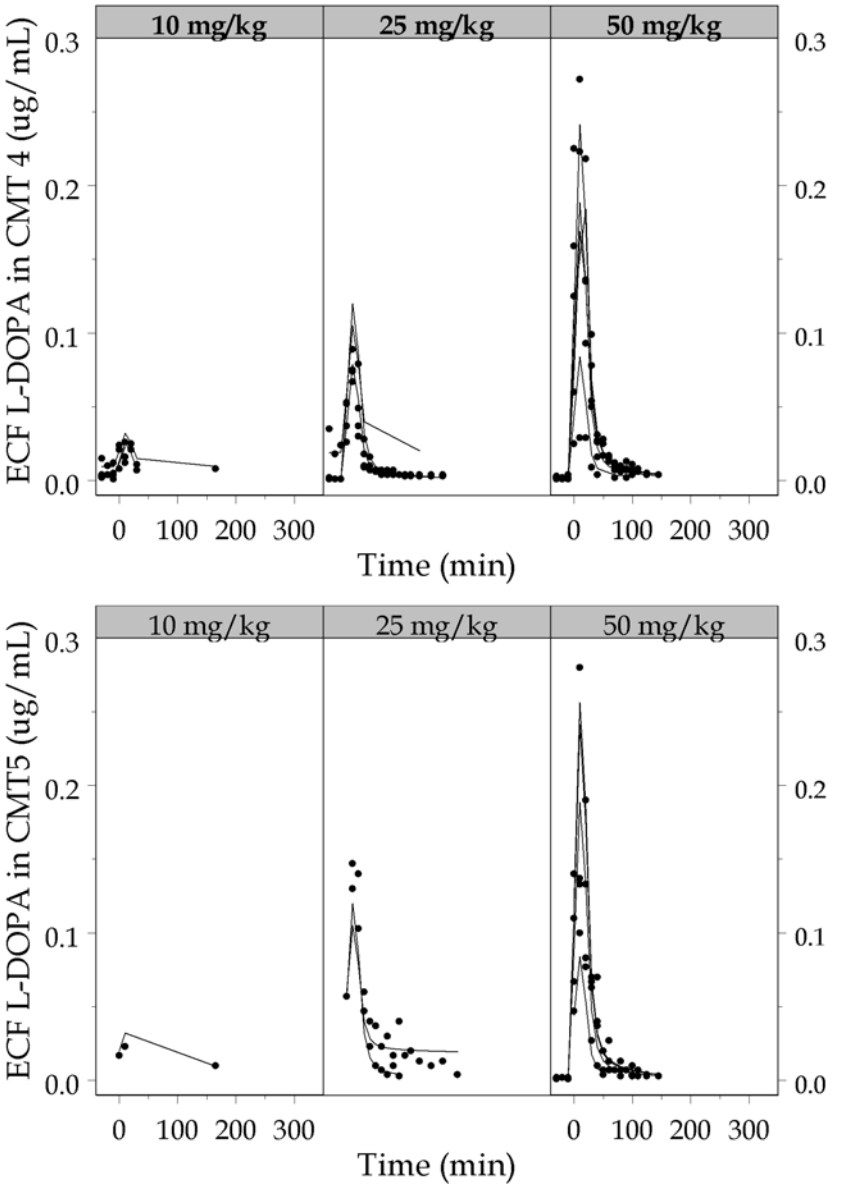

Figure 3: *L-DOPA concentration-time profiles in ECF in the untreated brain side (upper panel; in total 12 rats: 10 mg/kg: n=4; 25 mg/kg: n=3; 50 mg/kg: n=5) and in the lesioned brain side (lower panel; in total 7 rats: 10 mg/kg: n=1; 25 mg/kg: n=2; 50 mg/kg: n=4), obtained after a 20-min i.v. infusion in Lewis rats. Depicted are the observed concentrations (dots), individual predictions (solid lines), separated by L-DOPA dose.*

Table 1: *Population pharmacokinetic parameter estimates with the corresponding inter-individual coefficient of variation (CV%) and lower -and upper limit confidence intervals (LLCI and ULCI).*

Parameter	Estimate	CV%	LLCI-ULCI
L-DOPA			
Cl (mL/min)	30	21	17 – 43
ω^2 Cl	0.26	59	-0.041 – 0.56
V1 (mL)	98	39	24 – 172
V2 (mL)	157	15	112 – 202
V3 (mL)	599	15	425 – 773
V4 (mL)	13300	25	6810 – 19800
ω^2 V4	0.075	40	0.020 – 0.13
Q2 (mL/min)	22	24	11 – 32
Q3 (mL/min)	11	16	7.5 – 15
Q4 (mL/min)	22	14	16 – 29
Kin (min^{-1})	5.8	36	1.7 – 9.8
ω^2 Kin	0.94	41	0.19 – 1.7
Proportional error (plasma)	0.087	15	0.061 – 0.113
Proportional error (ECF)	0.17	21	0.10 – 0.24
UNTREATED BRAIN SIDE			
DOPAC			
k46 (min^{-1})	0.000044	28	0.000020 – 0.000068
ω^2 k46	0.50	60	-0.084 – 1.1
k40 (min^{-1})	0.53	23	0.29 – 0.77
ω^2 k40	0.42	46	0.045 – 0.80
k60 (min^{-1})	0.0053	17	0.0035 – 0.0071
ω^2 k60	0.19	58	-0.025 – 0.41
Residual error (additive)	0.0020	16	0.0014 – 0.0026
HVA			
k47(min^{-1})	0.000023	15	0.000016 – 0.000030
ω^2 k47	0.019	70	-0.0070 – 0.000030
k40 (min^{-1})	0.19	16	0.13 – 0.25
k70 (min^{-1})	0.0044	12	0.0033 – 0.0054
ω^2 k70	0.14	53	-0.006 – 0.28
Residual error (additive)	0.0028	24	0.0015 – 0.0041
LESIONED BRAIN SIDE			
DOPAC			
k58(min^{-1})	0.000054	51	-0.00000039 – 0.000011
ω^2 k58	1.0	40	0.23 – 1.9
k50(min^{-1})	0.36	55	-0.025 – 0.75
ω^2 k50	0.53	36	0.16 – 0.90
k80(min^{-1})	0.038	18	0.024 – 0.052
Residual error (additive)	0.0014	51	0.0000020 – 0.0027
HVA			
k59(min^{-1})	0.000016	42	0.0000028 – 0.000030
ω^2 k59	0.49	65	-0.14 – 1.12
k50(min^{-1})	0.14	55	-0.010 – 0.29
k90(min^{-1})	0.011	39	0.0027 – 0.020
Residual error (additive)	0.0034	41	0.00060 – 0.0061

Note: V5=V4, Q5=Q4 and k50=k40

population kinetic model for DOPAC as well as for HVA could be adequately estimated (Table 1). No dose-dependency was found in any of the parameters for DOPAC or HVA. For DOPAC, k46 and k58 (rate constants which describe the conversion of L-DOPA, via dopamine, to DOPAC) do not significantly differ, which means that there appears to be no effect of disease on the metabolism of L-DOPA via dopamine to DOPAC. The same can be said for HVA for which the values of k47 and k59 do not significantly differ. On the other hand, the elimination rate constants were found to be 7-fold and 2.5-fold higher in lesioned brain side compared to untreated side for DOPAC (k60 and k80) and HVA (k70 and k90), respectively.

Table 2: *Summary of goodness-of-fit based on the minimum value of objective function, of eight assumptions within the modelling of L-DOPA in plasma and brain*$_{ECF}$*. The assumption 'NONE' is where all parameters were estimated.*

Assumption	Results	*MVOF*	V4	V5	Q4	Q5	K40	K50
NONE	**general**	*-2814*	11100	16100	20.9	25.3	0.211	0.135
	SE		3840	6970	3.74	9.24	0.033	0.0132
	CV(%)		34.6	43.3	17.9	36.5	15.6	9.78
V5 = V4	**general**	*-2808*	12700		22.9	20.1	0.193	0.161
	SE		5700		4.33	7.13	0.0329	0.0185
	CV(%)		44.9		18.9	35.5	17	11.5
k50 = k40	**general**	*-2803*	13200	12000	20.1	26	0.175	
	SE		3870	4990	3.36	8.77	0.0226	
	CV(%)		29.3	41.6	16.7	33.7	12.9	
Q5 = Q4	**general**	*-2813*	11400	14400	22		0.211	0.135
	SE		3080	3700	3.18		0.027	0.0127
	CV(%)		27	25.7	14.5		12.8	9.41
V5 = V4 & k50 = k40	**general**	*-2804*	13000		21.4	24.3	0.179	
	SE		3410		3.2	5.56	0.0199	
	CV(%)		26.2		15	22.9	11.1	
V5 = V4 & Q5 = Q4	**general**	*m.t.*	13000		22		0.19	0.17
	SE		-	-	-	-	-	-
	CV(%)		-	-	-	-	-	-
k50 = k40 & Q5 = Q4	**general**	*-2801*	13900	10600	21.7		0.173	
	SE		8290	6610	7.79		0.0276	
	CV(%)		59.6	62.4	35.9		16	
V5 = V4 & k50 = k40 & Q5 = Q4	**general**	*-2801*	13300		22.4		0.175	
	SE		3310		3.17		0.0201	
	CV(%)		24.9		14.2		11.5	

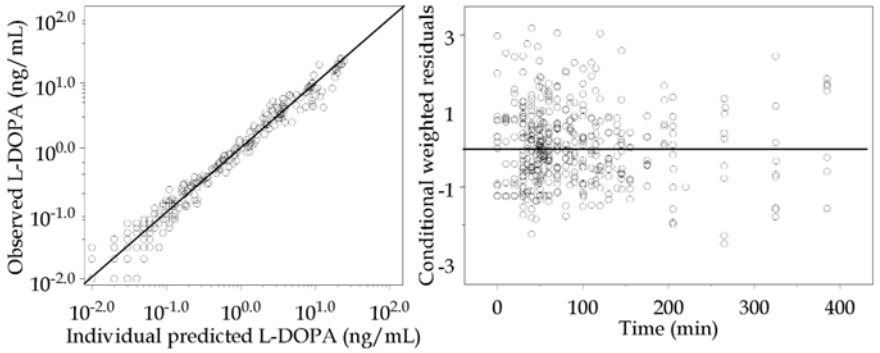

Figure 4: *Goodness-of-fit plots of L-DOPA concentrations in plasma and brainECF as described by the model depicted in Figure 1. The left panel depicts a scatterplot of the observed L-DOPA concentrations versus the individual model predictions. The line represents the line of unity. The right panel depicts a scatterplot of the conditional weighted residuals versus time.*

4. Discussion

In this study the relationship between plasma and $brain_{ECF}$ kinetics of L-DOPA and its conversion into the dopamine metabolites DOPAC and HVA was measured in rats, in parallel in the lesioned and untreated brain side, at 14 days post-rotenone injection. NONMEM was used to develop a population based PK model. Basal concentrations of DOPAC and HVA in striatal microdialysate differed between the lesioned and the untreated brain side. Furthermore, the model showed that without changes in BBB transport of L-DOPA, disease-related changes were observed in the kinetics of these dopamine metabolites following L-DOPA administration.

The results described in this paper are the first in which both plasma PK and $brain_{ECF}$ PK of L-DOPA in untreated and diseased (lesioned) conditions are described by one population PK model. The PK of L-DOPA in plasma following *i.v.* administration was best described by a three-compartmental model, like previously reported (Doller *at al*., 1978). In our study, we were not able to measure endogenous plasma concentrations of L-DOPA (LLQ was 1 µg/mL). Sato *et al* (1994a) found in their study in rats a basal level of 2.1 ± 0.6 mg/L. In our study, rats were fasted overnight which might be the reason for much lower endogenous L-DOPA in plasma. The total clearance of exogenous plasma in the study by Sato *et al* (1994a) was 3.13 L/h/kg which is in the same range as our value of 6.25 L/h/kg (Cl= 30 mL/min, Table 1; mean weight of the rats before start of the experiment was 288 ± 13g).

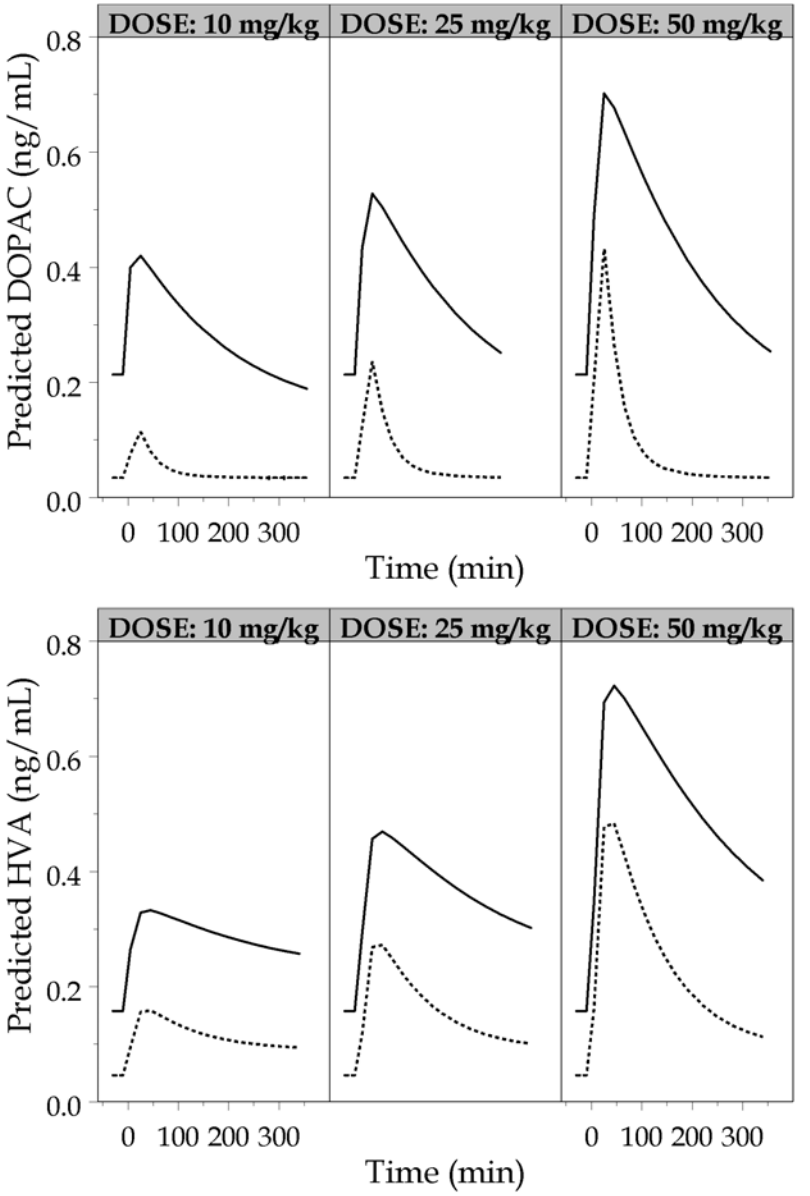

Figure 5: *Depicted are the population predicted concentrations of DOPAC (upper panel) and HVA (lower panel) in the untreated brain side (——) and lesioned brain side (- - -) according to the model as described in Figure 1, separated by L-DOPA dose. For each dose, a typical rat is depicted.*

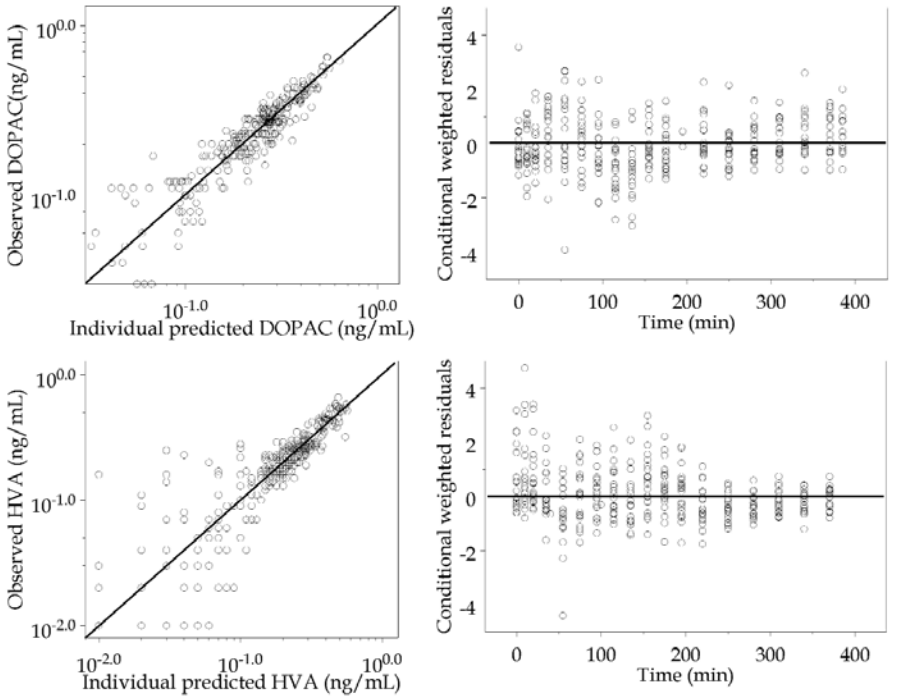

Figure 6: *Goodness-of-fit plots of DOPAC (upper panel) and HVA (lower panel) concentrations in microdialysate as described by the model depicted in Figure 1. The left graph of each panel depicts a scatterplot of the observed dialysate concentrations versus the individual model predictions. The line represents the line of unity. The right graph of each panel depicts a scatterplot of the weighted residuals versus time.*

In our study, following the rotenone infusion in the MFB, Parkinson's disease state was defined as a density of TH immunostaining in the striatum that was less than 40% of control (responders). Data indicated that the success of the model to induce neurodegeneration was similar to our previous study (Ravenstijn *at al.*, 2008), and the disease pathology was induced in about 70% of the rats. No difference in BBB transport of L-DOPA between the untreated and lesioned brain side were found. Also, our results did not indicate a disease-induced change in the endogenous production of L-DOPA in the brain (Kin; 5.8 min^{-1}). Since dopamine-producing neurons are diminished in Parkinson's disease (Dauer and Przedborski, 2003), one would expect a decrease in the endogenous concentration of L-DOPA, as it is a product of the metabolism of L-tyrosine by TH. However, it has been reported that TH enzyme activity, as a function of the degree of dopamine loss, is upregulated in the striatum of 6-OHDA lesioned rats and of

MPTP-treated rhesus monkeys (Pifl and Hornykiewicz, 2006). This phenomenon is assumed to be a compensatory mechanism of the remaining dopaminergic neurons triggered by the synaptic dopamine loss (Rose *at al.*, 1989). Upregulation of TH in the rotenone lesioned brain side seems therefore to explain our results.

Furthermore, the metabolism of L-DOPA via dopamine to DOPAC in the untreated brain (0.000044 min^{-1}) was indistinguishable from this metabolism in the lesioned brain side (0.000054 min^{-1}). Also, the metabolism of L-DOPA via dopamine to HVA in the untreated brain side (0.000023 min^{-1}) was similar to that in the lesioned brain side (0.000016 min^{-1}). These relatively low values, reflecting a slow conversion of L-DOPA via dopamine to these metabolites, is due to dopamine being the main metabolite of L-DOPA in the early phase after drug administration (Miwa *at al.*, 1992). Furthermore, this newly synthesised dopamine is localised exclusively in the intracellular compartment within this timeframe (DeJesus *at al.*, 2000; Miwa *at al.*, 1992). It is therefore not readily available for metabolism to DOPAC and/or HVA. Overall, in contrast to our expectations, it can be said that the disease conditions at 2 weeks post-rotenone-injection in the MFB did not result in any change in the kinetics of L-DOPA.

Differences for the dopamine metabolites DOPAC and HVA between lesioned and untreated brain side were observed for baseline concentrations as well as for elimination rate constants following L-DOPA administration, while their formation rate constants remained unaffected. The baseline concentrations of DOPAC and HVA were about 10-fold decreased in the lesioned brain side (Figure 5). These findings are similar to what has been reported in other studies in rats, after an intracerebral injection of rotenone into the MFB (Antkiewicz-Michaluk *at al.*, 2004), and intracerebral 6-OHDA injection (Brannan *at al.*, 1990; Sarre *at al.*, 1992). Such concentrations result from the rate of formation relative to that of elimination. As no changes in formation rate constants of DOPAC and HVA were found in the lesioned relative to the untreated brain side, decrease in baseline concentrations were the result of solely the increased elimination rate constants.

In our model, the metabolism from dopamine to DOPAC and HVA was explained by first-order kinetics (Figure 1, Table 1), like in the model previously developed (Sato *at al.*, 1994a; Sato *at al.*, 1994b). Following L-DOPA administration, for DOPAC, the elimination rate constant in the lesioned brain side (0.038 min^{-1}) was increased about 7-fold compared with the elimination rate constant in the untreated side (0.0053 min^{-1}). For HVA this disease-induced increase was about a factor 2.5 (0.011 min^{-1} for the lesioned versus 0.0044 min^{-1} for the untreated brain

side). Elimination of DOPAC from the ECF may occur by conjugation, in rats mostly to sulphates (Swahn and Wiesel, 1976) or by transformation to HVA by COMT. HVA is formed as metabolite of DOPAC but also directly from dopamine (Mannisto *at al.*, 1992; Westerink and de Vries, 1985; Wood and Altar, 1988). The mechanisms of elimination of HVA from the brain are not fully clear. HVA may leave the brain by passive diffusion (Amin *at al.*, 1992). Also, HVA effluxes from the brain via a probenecid-sensitive organic anion transport (OAT3) system, present at the BBB (Mori *at al.*, 2003). This HVA efflux transport system is likely to play an important role in controlling the level of HVA in the CNS. The apparent in vivo efflux rate constant of HVA from the brain was determined by (Mori *at al.*, 2003) to be 0.017 min^{-1}. Our value for the elimination rate constant of HVA in the untreated brain side was 0.044 min^{-1} and is in the same order of magnitude. The increased values that we found for the elimination rate constants for DOPAC and HVA could have been the result of upregulation of one of the active elimination processes. Though expressions of OATs are affected (mainly downregulated) in certain renal and hepatic diseases (Anzai *at al.*, 2006), to our knowledge, no studies have been performed indicating changes in OAT functionality at the BBB. However, even without the explanation of changes in functionality of the eliminating processes, the lower baseline values and increased elimination rates of DOPAC and HVA can be explained. In our study, the rate of formation of DOPAC and HVA is much lower than their rates of elimination (Table 1). The concept of "absorption-rate limited elimination" (Rowland and Tozer, 1995), that may occur when the absorption rate constant is significantly lower than the (true) elimination rate constant, might apply to our situation. In "absorption-rate limited elimination", the absorption process is very slow so that the product of the absorption rate constant and amount remaining to be absorbed approximately equals the product of the elimination rate constant and the amount to be eliminated ($k_a.A_a \sim k_{el}.A_{el}$). We propose for our results a "formation rate-limited elimination". Assuming identical distribution volumes for dopamine and its metabolites, the amounts can be divided by the distribution volume to give concentrations. As the formation rate constants of DOPAC and HVA are much lower than their corresponding elimination rate constants, the actual concentration of dopamine ("remaining to be metabolised") will govern the formation rate, and therewith the elimination rates of DOPAC and HVA. Then, $k_{form\ metabolite} * C_{dopamine} \sim k_{elim\ metabolite} * C_{metabolite}$. With unchanged values for formation of the metabolites ($k_{form\ metabolite}$ or k46 and k58 for DOPAC and k47 and k59 for HVA; see table 1), and lower baseline concentrations as measured

for both DOPAC and HVA, a higher (apparent) elimination rate constant is observed if dopamine concentrations would be lower in the lesioned brain side. This is indeed plausible with a diminished amount of dopaminergic neurons. This indicates that, though we have not been able to measure dopamine directly, the clearly lower baseline concentrations of DOPAC and HVA found in the lesioned brain side together with the increased values for the elimination rate constants, provides insight in changes in dopamine concentrations by the disease process.

We are the first to have developed a population PK model on the kinetics of L-DOPA, and its conversion on DOPAC and HVA in both untreated and (Parkinson's) lesioned brain. This opens up the possibility to further investigate the potential changes in the PK and conversion of L-DOPA at different stages of Parkinson's disease. Then, further investigations may focus on a potential relationship between a gradual decline in %TH staining and DOPAC and HVA microdialysate concentrations, which would give the opportunity to *in vivo* determine the Parkinson's disease state at multiple days as there is no need to sacrifice the experimental animal.

In conclusion, our study demonstrates that 2 weeks following a unilateral infusion of rotenone into the rat brain, there are no changes in the kinetics of L-DOPA in the lesioned hemisphere of the brain. However, a clear effect of dopamine depletion on the levels and elimination rates of DOPAC and HVA in brain was observed. This provides indirect information (confirmed by TH immunohistochemistry) for decreased dopamine concentrations at the lesioned brain side in accordance with "formation rate-limited elimination" PK principles. The models used here may help to unravel the molecular and biochemical mechanisms beyond the changes in the PK and its relation to the conversion of L-DOPA, in different stages of Parkinson's Disease. Further studies in other Parkinson's disease models that show progressive degeneration over time are warranted.

5. Reference List

Abbott NJ, Romero IA (1996). Transporting therapeutics across the blood-brain barrier. Mol. *Med. Today* 2: 106-113.

Alexander GM, Schwartzman RJ, Grothusen JR, Gordon SW (1994). Effect of plasma levels of large neutral amino acids and degree of parkinsonism on the blood-to-brain transport of levodopa in naive and MPTP parkinsonian monkeys. *Neurology* 44: 1491-1499.

Amin F, Davidson M, Davis KL (1992). Homovanillic acid measurement in clinical research: a review of methodology. *Schizophr. Bull.* 18: 123-148.

Antkiewicz-Michaluk L, Wardas J, Michaluk J, Romaska I, Bojarski A, Vetulani J (2004). Protective effect of 1-methyl-1,2,3,4-tetrahydroisoquinoline against dopaminergic neurodegeneration in the extrapyramidal structures produced by intracerebral injection of rotenone. *Int. J. Neuropsychopharmacol.* 7: 155-163.

Anzai N, Kanai Y, Endou H (2006). Organic anion transporter family: current knowledge. *J. Pharmacol. Sci.* 100: 411-426.

Bartels AL, Willemsen AT, Kortekaas R, de Jong BM, de Vries R, de Klerk O, van Oostrom JC, Portman A, Leenders KL (2008). Decreased blood-brain barrier P-glycoprotein function in the progression of Parkinson's disease, PSP and MSA. *J. Neural Transm.* 115: 1001-1009.

Bhidayasiri R, Truong DD (2008). Motor complications in Parkinson disease: clinical manifestations and management. *J. Neurol. Sci.* 266: 204-215.

Brannan T, Bhardwaj A, Martinez-Tica J, Weinberger J, Yahr M (1990). Striatal L-dopa metabolism studied in vivo in rats with nigrostriatal lesions. *J. Neural Transm. Park Dis. Dement.* Sect. 2: 15-22.

Carvey PM, Zhao CH, Hendey B, Lum H, Trachtenberg J, Desai BS, Snyder J, Zhu YG, Ling ZD (2005). 6-Hydroxydopamine-induced alterations in blood-brain barrier permeability. *Eur. J. Neurosci.* 22: 1158-1168.

Dauer W, Przedborski S (2003). Parkinson's disease: mechanisms and models. *Neuron* 39: 889-909.

de Lange EC, de Boer BA, Breimer DD (1999). Microdialysis for pharmacokinetic analysis of drug transport to the brain. *Adv. Drug Deliv. Rev.* 36: 211-227.

DeJesus OT, Haaparanta M, Solin O, Nickles RJ (2000). 6-fluoroDOPA metabolism in rat striatum: time course of extracellular metabolites. *Brain Res.* 877: 31-36.

del Amo EM, Urtti A, Yliperttula M (2008). Pharmacokinetic role of L-type amino acid transporters LAT1 and LAT2. *Eur. J. Pharm. Sci.* 35: 161-174.

Deleu D, Northway MG, Hanssens Y (2002). Clinical pharmacokinetic and pharmacodynamic properties of drugs used in the treatment of Parkinson's disease. *Clin. Pharmacokinet.* 41: 261-309.

Doller HJ, Connor JD, Lock DR, Sloviter RS, Dvorchik BH, Vesell ES (1978). Levodopa pharmacokinetics. Alterations after benserazide, a decarboxylase inhibitor. *Drug Metab Dispos.* 6: 164-168.

Factor SA (2008). Current status of symptomatic medical therapy in Parkinson's disease. *Neurotherapeutics.* 5: 164-180.

Hammarlund-Udenaes M (2000). The use of microdialysis in CNS drug delivery studies. Pharmacokinetic perspectives and results with analgesics and antiepileptics. *Adv. Drug Deliv. Rev.* 45: 283-294.

Kortekaas R, Leenders KL, van Oostrom JCH, Vaalburg W, Bart J, Willemsen ATM, Hendrikse NH (2005). Blood-Brain Barrier dysfunction in Parkinsonian midbrain in vivo. *Ann. Neurol.* 57: 176-179.

Mannisto PT, Ulmanen I, Lundstrom K, Taskinen J, Tenhunen J, Tilgmann C, Kaakkola S (1992). Characteristics of catechol O-methyl-transferase (COMT) and properties of selective COMT inhibitors. *Prog. Drug Res.* 39: 291-350.

Miwa S, Gillberg PG, Bjurling P, Yumoto N, Odano I, Watanabe Y, Langstrom B (1992). Assessment of dopamine and its metabolites in the intracellular and extracellular compartments of the rat striatum after peripheral administration of L-[11C]dopa. *Brain Res.* 578: 122-128.

Moghaddam B, Bunney BS (1989). Ionic composition of microdialysis perfusing solution alters the pharmacological responsiveness and basal outflow of striatal dopamine. *J. Neurochem.* 53: 652-654.

Mori S, Takanaga H, Ohtsuki S, Deguchi T, Kang YS, Hosoya K, Terasaki T (2003). Rat organic anion transporter 3 (rOAT3) is responsible for brain-to-blood efflux of homovanillic acid at the abluminal membrane of brain capillary endothelial cells. *J. Cereb. Blood Flow Metab* 23: 432-440.

Nutt JG, Woodward WR, Hammerstad JP, Carter JH, Anderson JL (1984). The "on-off" phenomenon in Parkinson's disease. Relation to levodopa absorption and transport. *N. Engl. J. Med.* 310: 483-488.

Nyholm D (2006). Pharmacokinetic optimisation in the treatment of Parkinson's disease : an update. *Clin. Pharmacokinet.* 45: 109-136.

Obeso JA, Rodriguez-Oroz M, Marin C, Alonso F, Zamarbide I, Lanciego JL, Rodriguez-Diaz M (2004). The origin of motor fluctuations in Parkinson's disease: importance of dopaminergic innervation and basal ganglia circuits. *Neurology* 62: S17-S30.

Paxinos G, Watson C, Pennisi M, Topple A (1985). Bregma, lambda and the interaural midpoint in

stereotaxic surgery with rats of different sex, strain and weight. *J. Neurosci. Methods* 13: 139-143.

Pifl C, Hornykiewicz O (2006). Dopamine turnover is upregulated in the caudate/putamen of asymptomatic MPTP-treated rhesus monkeys. *Neurochem. Int.* 49: 519-524.

Ravenstijn PG, Merlini M, Hameetman M, Murray TK, Ward MA, Lewis H, Ball G, Mottart C, de Ville dG, Lemarchand T, van Belle K, O'Neill MJ, Danhof M, de Lange EC (2008). The exploration of rotenone as a toxin for inducing Parkinson's disease in rats, for application in BBB transport and PK-PD experiments. *J. Pharmacol. Toxicol. Methods* 57: 114-130.

Rose S, Nomoto M, Kelly E, Kilpatrick G, Jenner P, Marsden CD (1989). Increased caudate dopamine turnover may contribute to the recovery of motor function in marmosets treated with the dopaminergic neurotoxin MPTP. *Neurosci. Lett.* 101: 305-310.

Rowland M & Tozer TN (1995). Extravascular Dose. In: ed. Balado,*D. Clinical Pharmacokinetics-Concepts and Applications.* Williams & Wilkins: Media, PA, pp 34-50.

Sarre S, Herregodts P, Deleu D, Devrieze A, De Klippel N, Ebinger G, Michotte Y (1992). Biotransformation of L-dopa in striatum and substantia nigra of rats with a unilateral, nigrostriatal lesion: a microdialysis study. *Naunyn Schmiedebergs Arch. Pharmacol.* 346: 277-285.

Sato S, Koitabashi T, Koshiro A (1994a). Pharmacokinetic and pharmacodynamic studies of L-dopa in rats. I. Pharmacokinetic analysis of L-dopa in rat plasma and striatum. *Biol. Pharm. Bull.* 17: 1616-1621.

Sato S, Koitabashi T, Koshiro A (1994b). Pharmacokinetic and pharmacodynamic studies of L-dopa in rats. II. Effect of L-dopa on dopamine and dopamine metabolite concentration in rat striatum. *Biol. Pharm. Bull.* 17: 1622-1629.

Savitt JM, Dawson VL, Dawson TM (2006). Diagnosis and treatment of Parkinson disease: molecules to medicine. *J. Clin. Invest* 116: 1744-1754.

Schapira AH (2008). Progress in neuroprotection in Parkinson's disease. *Eur. J. Neurol.* 15 Suppl 1: 5-13.

Swahn CG, Wiesel FA (1976). Determination of conjugated monoamine metabolites in brain tissue. *J. Neural Transm.* 39: 281-290.

Westerink BH, de Vries JB (1985). On the origin of dopamine and its metabolite in predominantly noradrenergic innervated brain areas. *Brain Res.* 330: 164-166.

Wood PL, Altar CA (1988). Dopamine release in vivo from nigrostriatal, mesolimbic, and mesocortical neurons: utility of 3-methoxytyramine measurements. *Pharmacol. Rev.* 40: 163-187.